

Slope stability analysis by finite elements

D. V. GRIFFITHS* and P. A. LANE†

The majority of slope stability analyses performed in practice still use traditional limit equilibrium approaches involving methods of slices that have remained essentially unchanged for decades. This was not the outcome envisaged when Whitman & Bailey (1967) set criteria for the then emerging methods to become readily accessible to all engineers. The finite element method represents a powerful alternative approach for slope stability analysis which is accurate, versatile and requires fewer *a priori* assumptions, especially, regarding the failure mechanism. Slope failure in the finite element model occurs ‘naturally’ through the zones in which the shear strength of the soil is insufficient to resist the shear stresses. The paper describes several examples of finite element slope stability analysis with comparison against other solution methods, including the influence of a free surface on slope and dam stability. Graphical output is included to illustrate deformations and mechanisms of failure. It is argued that the finite element method of slope stability analysis is a more powerful alternative to traditional limit equilibrium methods and its widespread use should now be standard in geotechnical practice.

KEYWORDS: dams; limit equilibrium methods; numerical modelling; plasticity; slopes.

INTRODUCTION

Elasto-plastic analysis of geotechnical problems using the finite element (FE) method has been widely accepted in the research arena for many years; however, its routine use in geotechnical practice for slope stability analysis still remains limited. The reason for this lack of acceptance is not entirely clear; however, advocates of FE techniques in academe must take some responsibility.

Manuscript received 28 May 1998; revised manuscript accepted 8 December 1998. Discussion on this paper closes 3 September 1999; for further details see p. ii.

* Colorado School of Mines, Golden.

† UMIST, Manchester.

En grande majorité, les analyses de stabilité de pente menées dans la pratique continuent à utiliser les méthodes traditionnelles d'équilibre limite et des systèmes de tranches qui n'ont pratiquement pas changé depuis des dizaines d'années. Ce n'était pas le résultat envisagé quand Whitman et Bailey (1967) ont établi des critères pour que ces méthodes alors émergentes puissent devenir facilement accessibles à tous les ingénieurs. La méthode d'éléments finis qui représente une alternative puissante pour les analyses de stabilité de pente, est exacte, polyvalente et demande moins d'hypothèses ‘a priori’, surtout en ce qui concerne les mécanismes de rupture. La rupture de pente dans le modèle à éléments finis se produit ‘naturellement’ à travers des zones dans lesquelles la résistance au cisaillement du sol est insuffisante pour résister aux contraintes tangentielles. Cet exposé décrit plusieurs exemples d'analyses de stabilité de pente utilisant les éléments finis et établit des comparaisons avec d'autres méthodes, comme l'influence d'une surface libre sur la stabilité d'une pente et d'une digue. Nous joignons une représentation graphique pour illustrer les déformations et mécanismes de rupture. Nous avançons que la méthode d'éléments finis pour analyser la stabilité des pentes constitue une alternative plus puissante aux méthodes traditionnelles d'équilibre limite et que son utilisation devrait maintenant devenir une pratique standard en géotechnique.

Practising engineers are often sceptical of the need for such complexity, especially in view of the poor quality of soil property data often available from routine site investigations. Although this scepticism is often warranted, there are certain types of geotechnical problem for which the FE approach offers real benefits. The challenge for an experienced engineer is to know which kind of problem would benefit from a FE treatment and which would not.

In general, linear problems such as the prediction of settlements and deformations, the calculation of flow quantities due to steady seepage or the study of transient effects due to consolidation are all highly amenable to solution by finite elements. Traditional approaches involving charts, tables or

graphical methods will often be adequate for routine problems but the FE approach may be valuable if awkward geometries or material variations are encountered which are not covered by traditional chart solutions.

The use of nonlinear analysis in routine geotechnical practice is harder to justify, because there is usually a significant increase in complexity which is more likely to require the help of a modelling specialist. Nonlinear analyses are inherently iterative in nature, because the material properties and/or the geometry of the problem are themselves a function of the 'solution'. Objections to nonlinear analyses on the grounds that they require excessive computational power, however, have been largely overtaken by developments in, and falling costs of, computer hardware. A desktop computer with a standard processor is now capable of performing nonlinear analyses such as those described in this paper in a reasonable time span—minutes rather than hours or days.

Slope stability represents an area of geotechnical analysis in which a nonlinear FE approach offers real benefits over existing methods. As this paper will show, slope stability analysis by elasto-plastic finite elements is accurate, robust and simple enough for routine use by practising engineers. Perception of the FE method as complex and potentially misleading is unwarranted and ignores the real possibility that misleading results can be obtained with conventional 'slip circle' approaches. The graphical capabilities of FE programs also allow better understanding of the mechanisms of failure, simplifying the output from reams of paper to manageable graphs and plots of displacements.

TRADITIONAL METHODS OF SLOPE STABILITY ANALYSIS

Most textbooks on soil mechanics or geotechnical engineering will include reference to several alternative methods of slope stability analysis. In a survey of equilibrium methods of slope stability analysis reported by Duncan (1996), the characteristics of a large number of methods were summarized, including the ordinary method of slices (Fellenius, 1936), Bishop's Modified Method (Bishop, 1955), force equilibrium methods (e.g. Lowe & Karafiath, 1960), Janbu's generalized procedure of slices (Janbu, 1968), Morgenstern and Price's method (Morgenstern & Price, 1965) and Spencer's method (Spencer, 1967).

Although there seems to be some consensus that Spencer's method is one of the most reliable, textbooks continue to describe the others in some detail, and the wide selection of available methods is at best confusing to the potential user. For example, the controversy was recently revisited by

Lambe & Silva (1995), who maintained that the ordinary method of slices had an undeservedly bad reputation.

A difficulty with *all* the equilibrium methods is that they are based on the assumption that the failing soil mass can be divided into slices. This in turn necessitates further assumptions relating to side force directions between slices, with consequent implications for equilibrium. The assumption made about the side forces is one of the main characteristics that distinguishes one limit equilibrium method from another, and yet is itself an entirely artificial distinction.

FINITE ELEMENT METHOD FOR SLOPE STABILITY ANALYSIS

Duncan's review of FE analysis of slopes concentrated mainly on deformation rather than stability analysis of slopes; however, attention was drawn to some important early papers in which elasto-plastic soil models were used to assess stability. Smith & Hobbs (1974) reported results of $\phi_u = 0$ slopes and obtained reasonable agreement with Taylor's (1937) charts. Zienkiewicz *et al.* (1975) considered a c' , ϕ' slope and obtained good agreement with slip circle solutions. Griffiths (1980) extended this work to show reliable slope stability results over a wide range of soil properties and geometries as compared with charts of Bishop & Morgenstern (1960). Subsequent use of the FE method in slope stability analysis has added further confidence in the method (e.g. Griffiths, 1989; Potts *et al.*, 1990; Matsui & San, 1992). Duncan mentions the potential for improved graphical results and reporting utilizing FE, but cautions against artificial accuracy being assumed when the input parameters themselves are so variable.

Wong (1984) gives a useful summary of potential sources of error in the FE modelling of slope stability, although recent results, including those presented in this paper, indicate that better accuracy is now possible.

Advantages of the finite element method

The advantages of a FE approach to slope stability analysis over traditional limit equilibrium methods can be summarized as follows:

- (a) No assumption needs to be made in advance about the shape or location of the failure surface. Failure occurs 'naturally' through the zones within the soil mass in which the soil shear strength is unable to sustain the applied shear stresses.
- (b) Since there is no concept of slices in the FE approach, there is no need for assumptions about slice side forces. The FE method

preserves global equilibrium until 'failure' is reached.

- (c) If realistic soil compressibility data are available, the FE solutions will give information about deformations at working stress levels.
- (d) The FE method is able to monitor progressive failure up to and including overall shear failure.

Brief description of the finite element model

The programs used in this paper are based closely on Program 6.2 in the text by Smith & Griffiths (1998), the main difference being the ability to model more general geometries and soil property variations, including variable water levels and pore pressures. Further graphical output capabilities have been added. The programs are for two-dimensional plane strain analysis of elastic–perfectly plastic soils with a Mohr–Coulomb failure criterion utilizing eight-node quadrilateral elements with reduced integration (four Gauss points per element) in the gravity loads generation, the stiffness matrix generation and the stress redistribution phases of the algorithm. The soil is initially assumed to be elastic and the model generates normal and shear stresses at all Gauss points within the mesh. These stresses are then compared with the Mohr–Coulomb failure criterion. If the stresses at a particular Gauss point lie within the Mohr–Coulomb failure envelope, then that location is assumed to remain elastic. If the stresses lie on or outside the failure envelope, then that location is assumed to be yielding. Yielding stresses are redistributed throughout the mesh utilizing the visco-plastic algorithm (Perzyna, 1966; Zienkiewicz & Cormeau, 1974). Overall shear failure occurs when a sufficient number of Gauss points have yielded to allow a mechanism to develop.

The analyses presented in this paper do not attempt to model tension cracks. Although 'no-tension' criteria can be incorporated into elasto-plastic FE analyses (e.g. Naylor & Pande, 1981), this additional constraint on stress levels complicates the algorithm, and, in addition, there is still some debate as to how 'tension' should properly be defined. Further research in this area is warranted.

Soil model

The soil model used in this study consists of six parameters, as shown in Table 1.

The dilation angle ψ affects the volume change of the soil during yielding. It is well known that the actual volume change exhibited by a soil during yielding is quite variable. For example, a medium–dense material during shearing might initially exhibit some volume decrease ($\psi < 0$),

Table 1. Six-parameter soil model

ϕ'	Friction angle
c'	Cohesion
ψ	Dilation angle
E'	Young's modulus
ν'	Poisson's ratio
γ	Unit weight

followed by a dilative phase ($\psi > 0$), leading eventually to yield under constant volume conditions ($\psi = 0$). Clearly, this type of detailed volumetric modelling is beyond the scope of the elastic–perfectly plastic models used in this study, where a constant dilation angle is implied.

The question then arises as to what value of ψ to use. If $\psi = \phi$, then the plasticity flow rule is 'associated' and direct comparisons with theorems from classical plasticity can be made. It is also the case that when the flow rule is associated, the stress and velocity characteristics coincide, so closer agreement can be expected between failure mechanisms predicted by finite elements and critical failure surfaces generated by limit equilibrium methods.

In spite of these potential advantages of using an associated flow rule, it is also well known that associated flow rules with frictional soil models predict far greater dilation than is ever observed in reality. This in turn leads to increased failure load prediction, especially in 'confined' problems such as bearing capacity (Griffiths, 1982). This shortcoming has led some of the most successful constitutive soil models to incorporate non-associated plasticity (e.g. Molenkamp, 1981; Hicks & Bougharou, 1998).

Slope stability analysis is relatively unconfined, so the choice of dilation angle is less important. As the main objective of the current study is the accurate prediction of slope factors of safety, a compromise value of $\psi = 0$, corresponding to a non-associated flow rule with zero volume change during yield, has been used throughout this paper. It will be shown that this value of ψ enables the model to give reliable factors of safety and a reasonable indication of the location and shape of the potential failure surfaces.

The parameters c' and ϕ' refer to the effective cohesion and friction angle of the soil. Although a number of failure criteria have been suggested for modelling the strength of soil (e.g. Griffiths, 1990), the Mohr–Coulomb criterion remains the one most widely used in geotechnical practice and has been used throughout this paper. In terms of principal stresses and assuming a compression–negative sign convention, the criterion can be written as follows:

$$F = \frac{\sigma'_1 + \sigma'_3}{2} \sin \phi' - \frac{\sigma'_1 - \sigma'_3}{2} - c' \cos \phi' \quad (1)$$

where σ'_1 and σ'_3 are the major and minor principal effective stresses.

The failure function F can be interpreted as follows:

- $F < 0$ stresses inside failure envelope (elastic)
- $F = 0$ stresses on failure envelope (yielding)
- $F > 0$ stresses outside failure envelope (yielding and must be redistributed)

The elastic parameters E' and ν' refer to Young's modulus and Poisson's ratio of the soil. If a value of Poisson's ratio is assumed (typical drained values lie in the range $0.2 < \nu' < 0.3$), the value of Young's modulus can be related to the compressibility of the soil as measured in a one-dimensional oedometer (e.g. Lambe & Whitman, 1969):

$$E' = \frac{(1 + \nu')(1 - 2\nu')}{m_v(1 - \nu')} \quad (2)$$

where m_v is the coefficient of volume compressibility.

Although the actual values given to the elastic parameters have a profound influence on the computed deformations prior to failure, they have little influence on the predicted factor of safety in slope stability analysis. Thus, in the absence of meaningful data for E' and ν' , they can be given nominal values (e.g. $E' = 10^5$ kN/m² and $\nu' = 0.3$).

The total unit weight γ assigned to the soil is proportional to the nodal self-weight loads generated by gravity.

In summary, the most important parameters in a FE slope stability analysis are the same as they would be in a traditional approach, namely, the total unit weight γ , the shear strength parameters c' and ϕ' , and the geometry of the problem.

Gravity loading

The forces generated by the self-weight of the soil are computed using a standard gravity 'turn-on' procedure involving integrals over each element of the form:

$$\mathbf{p}^{(e)} = \gamma \int_{V^e} \mathbf{N}^T d(\text{vol}) \quad (3)$$

where \mathbf{N} values are the shape functions of the element and the superscript e refers to the element number. This integral evaluates the area of each element, multiplies by the total unit weight of the soil and distributes the net vertical force consist-

tently to all the nodes. These element forces are assembled into a global gravity force vector that is applied to the FE mesh in order to generate the initial stress state of the problem.

The present work applies gravity in a single increment to an initially stress-free slope. Others have shown that under elastic conditions, sequential loading in the form of incremental gravity application or embanking affects deformations but not stresses (e.g. Clough & Woodward, 1967). In non-linear analyses, it is recognized that the stress paths followed due to sequential excavation may be quite different to those followed under a gravity 'turn-on' procedure; however, the factor of safety appears unaffected when using simple elasto-plastic models (e.g. Borja *et al.* 1989; Smith & Griffiths, 1998).

In comparing our results with limit equilibrium solutions which generally take no account of loading sequence, our experience has shown that the predicted factor of safety is insensitive to the form of gravity application when using elastic–perfectly plastic Mohr–Coulomb models. An example of this insensitivity is demonstrated later in the paper.

The factor of safety may be sensitive to loading sequence when implementing more complex constitutive laws, such as those that attempt to reproduce volumetric changes accurately in an undrained or partially drained environment. For example, Hicks & Wong (1988) showed that the effective stress path could have a big influence on the factor of safety of an undrained slope.

Determination of the factor of safety

The factor of safety (FOS) of a soil slope is defined here as the number by which the original shear strength parameters must be divided in order to bring the slope to the point of failure. (This definition of the factor of safety is exactly the same as that used in traditional limit equilibrium methods, namely the ratio of restoring to driving moments.) The factored shear strength parameters c'_f and ϕ'_f , are therefore given by:

$$c'_f = c' / \text{FOS} \quad (4)$$

$$\phi'_f = \arctan \left(\frac{\tan \phi'}{\text{FOS}} \right) \quad (5)$$

This method has been referred to as the 'shear strength reduction technique' (e.g. Matsui & San, 1992) and allows for the interesting option of applying different factors of safety to the c' and $\tan \phi'$ terms. In this paper, however, the same factor is always applied to both terms. To find the 'true' FOS, it is necessary to initiate a systematic search for the value of FOS that will just cause the slope to fail. This is achieved by the program

solving the problem repeatedly using a sequence of user-specified FOS values.

Definition of failure

There are several possible definitions of failure, e.g. some test of bulging of the slope profile (Snitbhan & Chen, 1976), limiting of the shear stresses on the potential failure surface (Duncan & Dunlop, 1969) or non-convergence of the solution (Zienkiewicz & Taylor, 1989). These are discussed in Abramson *et al.* (1995) from the original paper by Wong (1984) but without resolution. In the examples studied here, the non-convergence option is taken as being a suitable indicator of failure.

When the algorithm cannot converge within a user-specified maximum number of iterations, the implication is that no stress distribution can be found that is simultaneously able to satisfy both the Mohr–Coulomb failure criterion and global equilibrium. If the algorithm is unable to satisfy these criteria, 'failure' is said to have occurred. Slope failure and numerical non-convergence occur simultaneously, and are accompanied by a dramatic increase in the nodal displacements within the mesh. Most of the results shown in this paper used an iteration ceiling of 1000 and are presented in the form of a graph of FOS versus $E'\delta_{\max}/\gamma H^2$ (a dimensionless displacement), where δ_{\max} is the maximum nodal displacement at convergence and H is the height of the slope. This graph may be used alongside the displaced mesh and vector plots to indicate both the factor of safety and the nature of the failure mechanism.

SLOPE STABILITY EXAMPLES AND VALIDATION

Several examples of FE slope stability analysis are now presented with validation against tradi-

tional stability analyses where possible. Initial consideration will be given to slopes containing no pore pressures in which total and effective stresses are equal. This is followed by examples of inhomogeneous undrained clay slopes. Finally, submerged and partially submerged slopes are considered in which pore pressures are taken into account.

Example 1: Homogeneous slope with no foundation layer ($D = 1$)

(See Fig. 5 for the definition of D .) The homogeneous slope shown in Fig. 1 has the following soil properties:

$$\phi' = 20^\circ$$

$$c'/\gamma H = 0.05$$

The slope is inclined at an angle of 26.57° (2:1) to the horizontal, and the boundary conditions are given as vertical rollers on the left boundary and full fixity at the base. Gravity loads were applied to the mesh and the trial factor of safety (FOS) gradually increased until convergence could not be achieved within the iteration limit as shown in Table 2.

The table indicates that six trial factors of safety were attempted, ranging from 0.8 to 1.4. Each factor of safety represented a completely independent analysis in which the soil strength parameters were scaled by FOS as indicated in equations (4) and (5). Some efficiencies are possible in that the gravity loads and global stiffness matrix are the same in each analysis and are therefore generated once only.

The 'Iterations' column indicates the number of iterations for convergence corresponding to each FOS value. The algorithm has to work harder to achieve convergence as the 'true' FOS is approached.

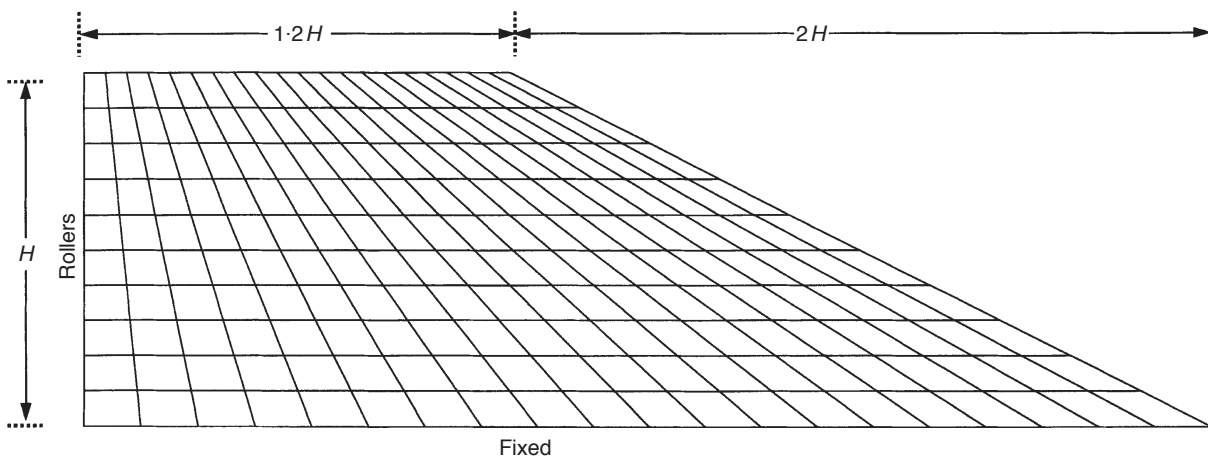


Fig. 1. Example 1: Mesh for a homogeneous slope with a slope angle of 26.57° (2:1), $\phi' = 20^\circ$, $c'/\gamma H = 0.05$

Table 2. Results from example 1

FOS	$E'\delta_{\max}/\gamma H^2$	Iterations
0.80	0.379	2
1.00	0.381	10
1.20	0.422	20
1.30	0.453	41
1.35	0.544	792
1.40	1.476	1000

When $FOS = 1.4$, there is a sudden increase in the dimensionless displacement $E'\delta_{\max}/\gamma H^2$, and the algorithm is unable to converge within the iteration limit. Fig. 2 shows a plot of the data from Table 2, and indicates close agreement between the FE result and the factor of safety given for the same problem by the charts of Bishop & Morgenstern (1960).

Figure 3 shows the influence of gravity loading increment size on displacements in example 1. With a 'failure' factor of safety of $FOS = 1.4$ applied to the soil properties, the four graphs correspond to the maximum displacement obtained when gravity was applied in a single increment as compared with that obtained with two, three or five equal increments. The figure demonstrates that the displacement obtained with full gravity loading is barely affected by the increment size.

Figures 4(a) and 4(b) give the nodal displacement vectors and the deformed mesh corresponding

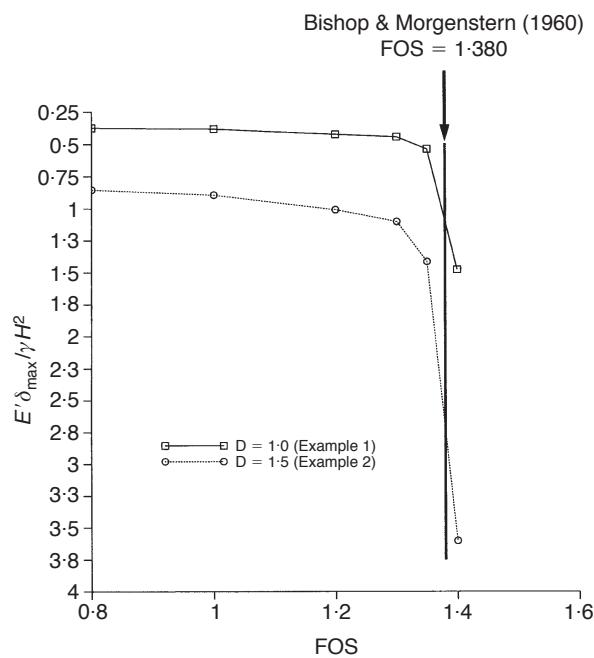


Fig. 2. Examples 1 and 2: FOS versus dimensionless displacement. The rapid increase in displacement and the lack of convergence when $FOS = 1.4$ indicates slope failure

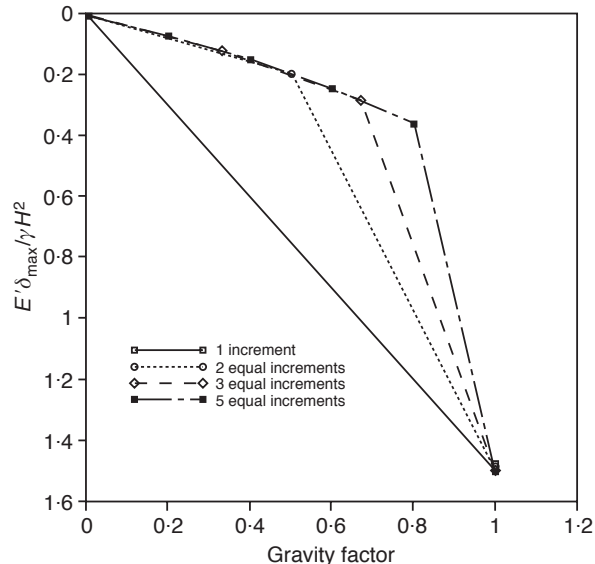


Fig. 3. Influence of gravity increment size on maximum displacement at failure ($FOS = 1.4$) from example 1

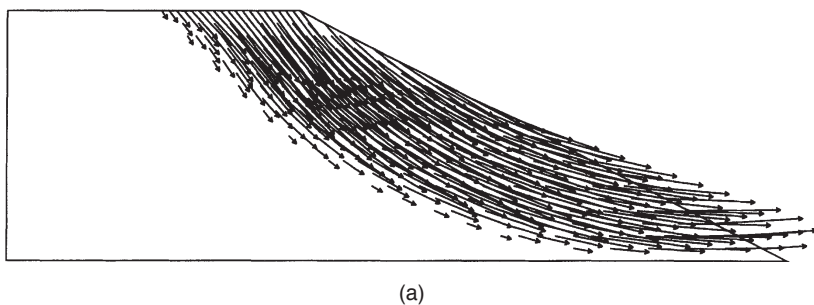
to the unconvolved situation with $FOS = 1.4$. The deformed mesh corresponding to this unconvolved solution gives a rather diffuse indication of the failure mechanism. This is due to the relatively crude FE mesh, which must remain continuous even at 'failure'. Conventional FE analysis is unable to model gross discontinuities along potential failure surfaces, although techniques have been described for enhancing the visualization of the failure surfaces (e.g. Griffiths & Kidger, 1995). More advanced FE methods for modelling shear bands in conjunction with adaptive mesh refinement techniques have been described by Loret & Prevost (1991) and Zienkiewicz *et al.* (1995).

Example 2: Homogeneous slope with a foundation layer ($D = 1.5$)

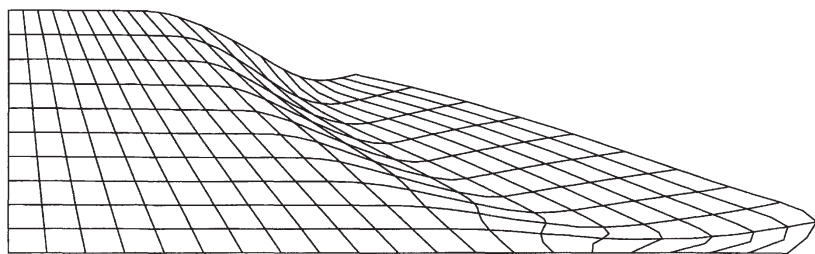
Figure 5 shows that a foundation layer of thickness $H/2$ has now been added to the base of the slope of example 1, with all other properties and geometry remaining the same.

The initial mesh and the deformed mesh at failure are shown in Figs 5(a) and 5(b) respectively. It is clear from Fig. 5(b) that a mechanism of the 'toe failure' type has been obtained. Fig. 2 indicates that the critical factor of safety is essentially unchanged from example 1 at $FOS = 1.4$, although the displacements are increased due to the greater volume of compressible soil.

This FE result confirms that the addition of the foundation layer has *not* led to any perceptible change in the factor of safety of the slope. Bishop & Morgenstern (1960) give $FOS = 1.752$ as one

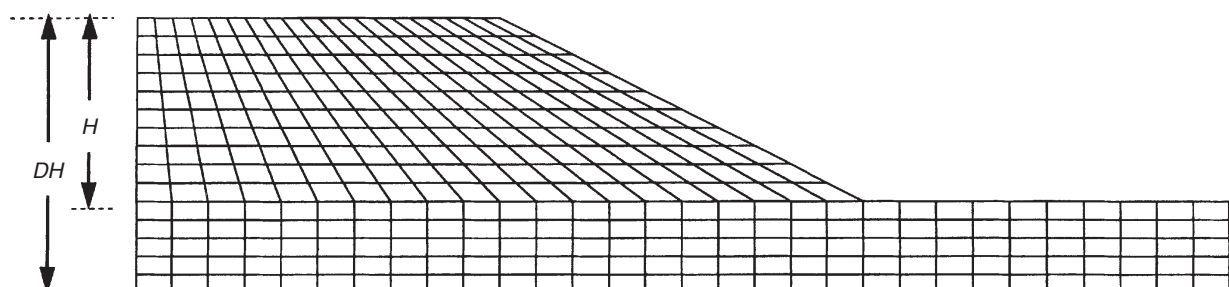


(a)

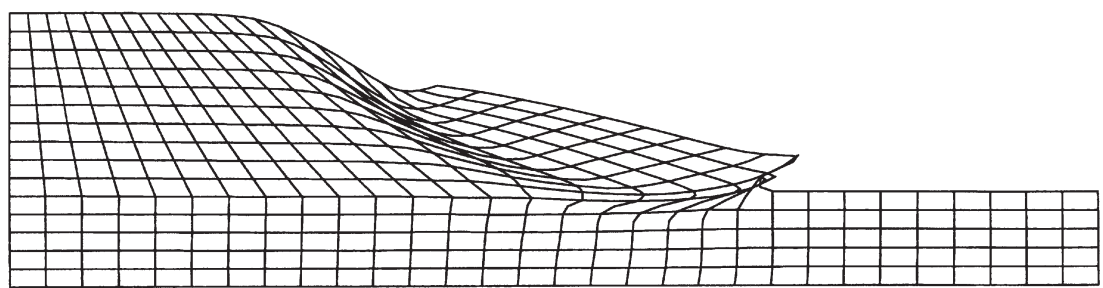


(b)

Fig. 4. Example 1: Deformed mesh plots corresponding to the un converged solution with FOS = 1.4: (a) nodal displacement vectors; (b) deformed mesh



(a)



(b)

Fig. 5. Example 2: Homogeneous slope with a foundation layer. Slope angle 26.57° (2:1), $\phi' = 20^\circ$, $c'/\gamma H = 0.05$, $D = 1.5$: (a) undeformed mesh; (b) mesh corresponding to un converged solution with FOS = 1.4

possible solution for this example ($D = 1.5$, $c'/(\gamma H) = 0.05$, $\phi' = 20^\circ$, 2:1 slope), although it is important to check the alternative solution corresponding to $D = 1.0$ to verify which gives the lower FOS. The charts of Cousins (1978) essentially agree with the FE result and indicate that, with a foundation layer, the critical circular mechanism at its lowest point passes fractionally below the base of the slope and gives a slightly lower factor of safety than when there is no foundation layer present.

Solving this example using a proprietary slip circle program also found the possible 'result' of FOS = 1.7 when a failure circle tangent to the base of the foundation was assumed. It was necessary to force the slip circle to pass through the toe to obtain the 'correct' FOS of 1.4.

This example demonstrates one of the main advantages of FE slope stability analysis over conventional methods. The FE approach requires no *a priori* assumption of the location or shape of the critical surface. Failure occurs 'naturally' within the zones of the soil mass where the shear strength of the soil is insufficient to resist the shear stresses. The use of a limit equilibrium method requires, at the very least, some experience and care on the part of the user in order to initiate appropriate search procedures which avoid the possibility of homing in on the wrong 'critical' circle.

Example 3: An undrained clay slope with a thin weak layer

The next example demonstrates a stability analysis of a slope of undrained clay. Effective stress analysis of an undrained slope of this type could

be performed with respect to effective stresses by adding a large apparent fluid bulk modulus to the soil constitutive matrix (Naylor, 1974). In this case, however, a total stress analysis using a Tresca failure criterion ($\phi_u = 0$) is presented.

Figure 6 shows a slope on a foundation layer ($D = 2$) of undrained clay. The slope includes a thin layer of weaker material which initially runs parallel to the slope, then horizontally in the foundation and finally outcrops at an angle of 45° beyond the toe. Although this example may seem contrived, it is not unlike the situation of a thin, weak liner within a landfill system. The factor of safety of the slope was estimated by FE analysis for a range of values of the undrained shear strength of the thin layer (c_{u2}) while maintaining the strength of the surrounding soil at $c_{u1}/\gamma H = 0.25$.

The FE results shown in Fig. 7 give the computed factor of safety expressed to the nearest 0.05. For a homogeneous slope ($c_{u2}/c_{u1} = 1$), the computed factor of safety was close to the Taylor solution (Taylor, 1937) of FOS = 1.47 and gave the expected circular base failure mechanism. As the strength of the thin layer was gradually reduced, a distinct change in the nature of the results was observed when $c_{u2}/c_{u1} \approx 0.6$.

Also shown on this figure are limit equilibrium solutions obtained using Janbu's method assuming both circular (base failure) and three-line wedge mechanisms following the path of the weak layer. The discontinuity when $c_{u2}/c_{u1} \approx 0.6$ clearly represents the transition between the circular mechanism and the non-circular mechanism governed by the weak layer. For $c_{u2}/c_{u1} > 0.6$, the (circular) base failure mechanism governs the behaviour, and

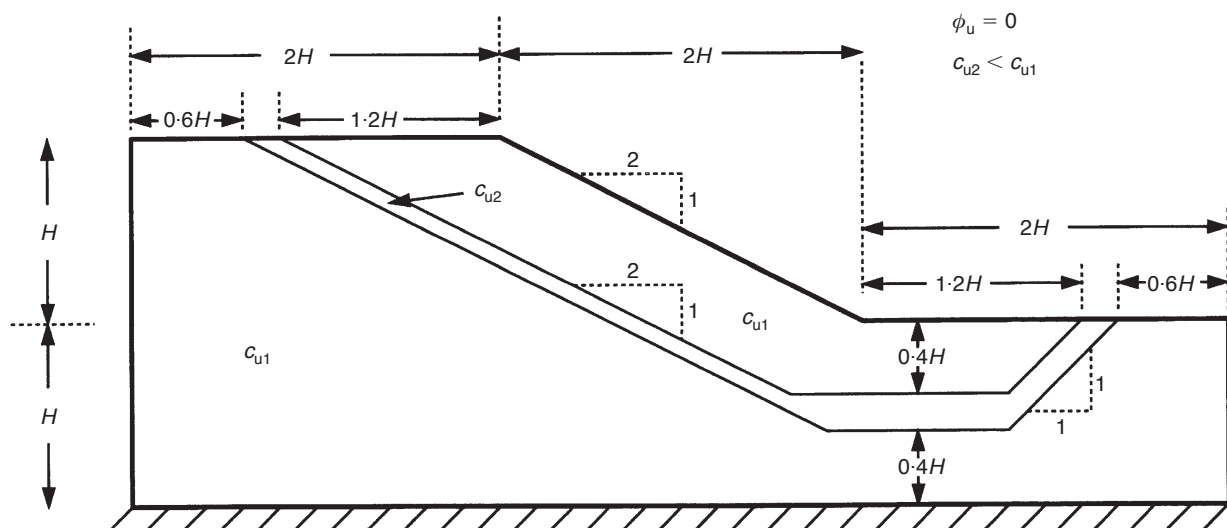


Fig. 6. Example 3: Undrained clay slope with a foundation layer including a thin weak layer ($D = 2$, $c_{u1}/\gamma H = 0.25$)

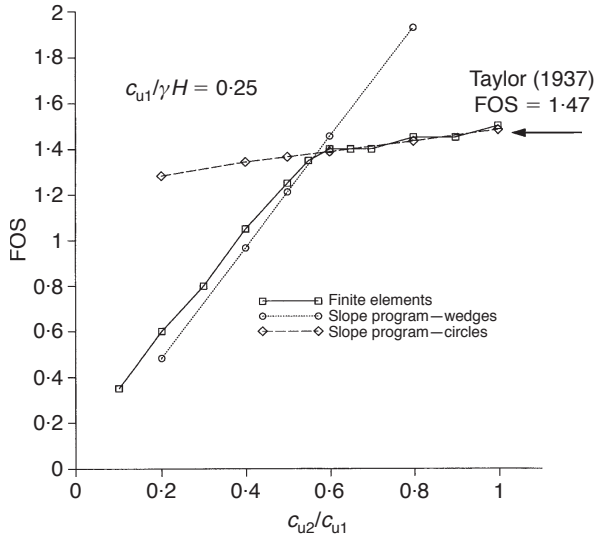


Fig. 7. Example 3: Computed factor of safety (FOS) for different values of c_{u2}/c_{u1}

the factor of safety is essentially unaffected by the strength of the weaker thin layer. For $c_{u2}/c_{u1} < 0.6$, the (non-circular) thin layer mechanism takes over and the factor of safety falls linearly.

This behaviour is explained more clearly in Fig. 8, which shows the deformed mesh at failure for three different values of the ratio c_{u2}/c_{u1} . Fig. 8(a), corresponding to the homogeneous case ($c_{u2}/c_{u1} = 1$), indicates an essentially circular failure mechanism tangent to the firm base as predicted by Taylor. Fig. 8(c), in which the strength of the thin layer is only 20% of that of the surrounding soil ($c_{u2}/c_{u1} = 0.2$), indicates a highly concentrated non-circular mechanism closely following the path of the thin weak layer. Fig. 8(b), in which the strength of the thin layer is 60% of that of the surrounding soil ($c_{u2}/c_{u1} = 0.6$), indicates considerable complexity and ambiguity. At least two conflicting mechanisms are apparent. First, there is a base failure mechanism merging

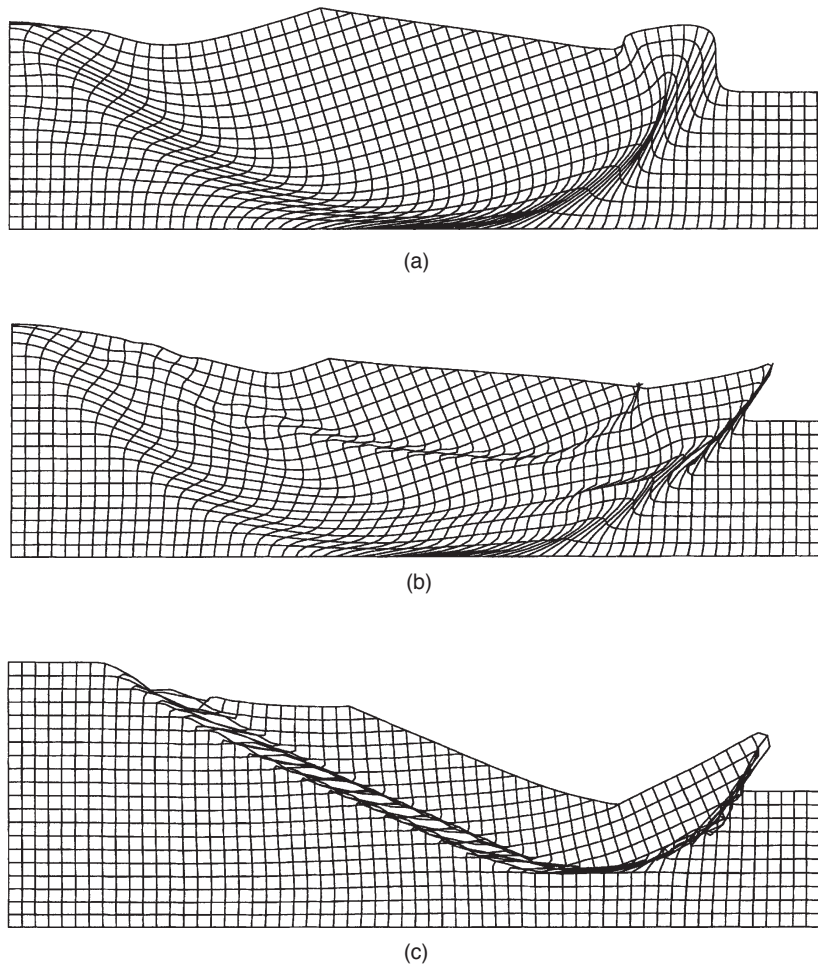


Fig. 8. Example 3: Deformed meshes at failure corresponding to the un-converged solution for three different values of c_{u2}/c_{u1} (a) $c_{u2}/c_{u1} = 1.0$; (b) $c_{u2}/c_{u1} = 0.6$; (c) $c_{u2}/c_{u1} = 0.2$

with the weak layer beyond the toe of the slope, and second, there is a mechanism running along the weak layer parallel to the slope and outcropping at the toe.

Without prior knowledge of the two alternative mechanisms, a traditional limit equilibrium search could seriously overestimate the factor of safety. This is illustrated in Fig. 7 where, for example, a circular mechanism with $c_{u2}/c_{u1} = 0.2$ would indicate $FOS = 1.3$, when the correct factor of safety is closer to 0.6.

Example 4: An undrained clay slope with a weak foundation layer

In this case, the same slope geometry and finite element mesh as in the previous example has been used but with a different type of inhomogeneity, as shown in Fig. 9. The shear strength of the slope material has been maintained at a constant value of $c_{u1}/\gamma H = 0.25$, while the shear strength of the foundation layer has been varied. The relative size of the two shear strengths has again been expressed as the ratio c_{u2}/c_{u1} . Fig. 10 shows the computed factor of safety for a range of c_{u2}/c_{u1} values, together with classical solutions of Taylor for the two cases when $c_{u2} = c_{u1}$ and $c_{u2} \gg c_{u1}$. There is clearly a change of behaviour occurring at $c_{u2}/c_{u1} \approx 1.5$, as indicated by the flattening out of the curve. Also shown on this figure are limit equilibrium solutions for both toe and base circle mechanisms. The discontinuity corresponding to $c_{u2}/c_{u1} \approx 1.5$ obviously represents the transition between these two fundamental mechanisms.

This transition is clearly demonstrated by the FE failure mechanisms shown in Fig. 11. When $c_{u2} \ll c_{u1}$ (Fig. 11(a)), a deep-seated base mechanism is observed (Fig. 11(a)), whereas a shallow 'toe' mechanism is seen when $c_{u2} \gg c_{u1}$ (Fig. 11(c)). The result corresponding to the approximate transition point at $c_{u2} \approx 1.5c_{u1}$ (Fig. 11(b)) shows

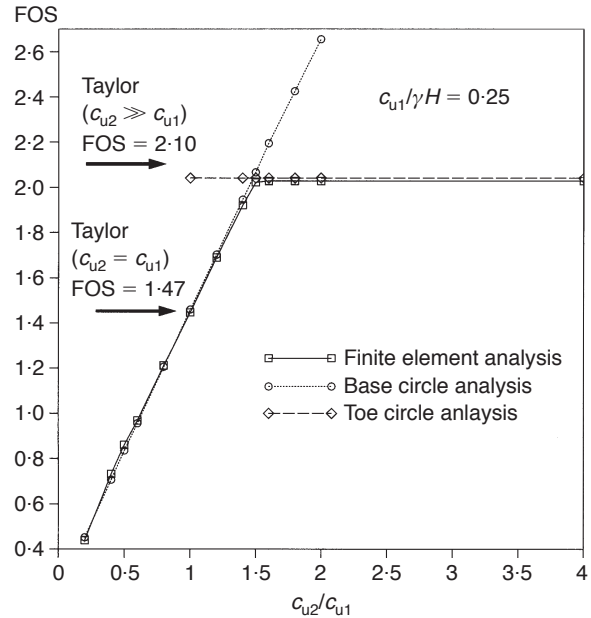


Fig. 10. Example 4: Computed factor of safety (FOS) for different values of c_{u2}/c_{u1}

an ambiguous situation in which both mechanisms are trying to form at the same time. It is interesting to note that the lower soil must be approximately 50% stronger than the upper soil before the toe mechanism becomes the most critical.

The previous two examples have shown that even in quite simple cases, complex interactions can occur between conflicting mechanisms within heterogeneous slopes which can be detected by the FE approach. For more complicated stability problems involving several soil property groups such as a zoned earth embankment, the FE approach is arguably the *only* rational method that will generate the correct factor of safety and indicate the location and shape of the critical mechanism.

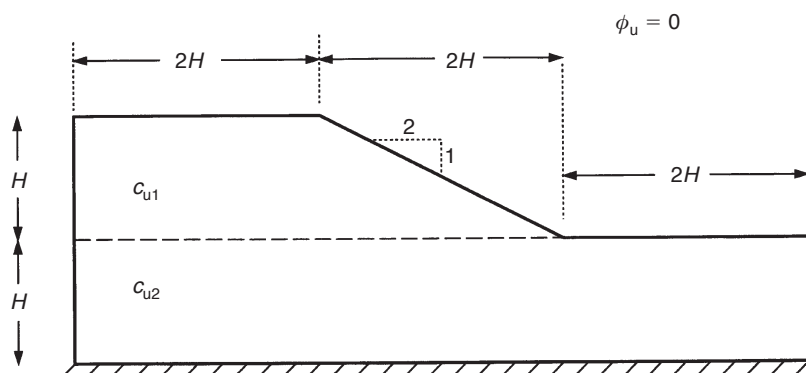


Fig. 9. Example 4: Undrained clay slope with a weak foundation layer ($D = 2$, $c_{u1}/\gamma H = 0.25$)

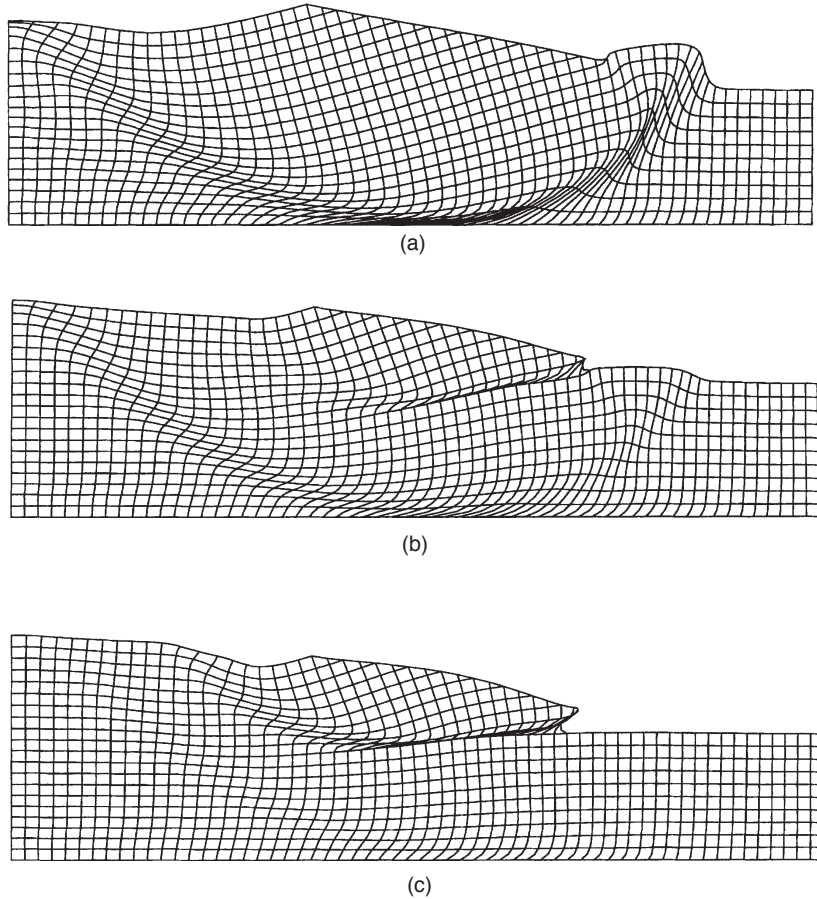


Fig. 11. Example 4: Deformed meshes at failure corresponding to the un converged solution for three different values of c_{u2}/c_{u1} : (a) $c_{u2}/c_{u1} = 0.6$; (b) $c_{u2}/c_{u1} = 1.5$; (c) $c_{u2}/c_{u1} = 2.0$

INFLUENCE OF FREE SURFACE AND RESERVOIR LOADING ON SLOPE STABILITY

We now consider the influence of a free surface within an earth slope and reservoir loading on the outside of a slope as shown in Fig. 12.

Regarding the role of the free surface, a rigorous approach would first involve obtaining a good-quality flow net for free surface flow through the slope, enabling pore pressures to be accurately estimated at any point within the flow region. For the purposes of slope stability analysis, however, it is usually considered sufficiently accurate and conservative to estimate pore pressure at a point as the product of the unit weight of water (γ_w) and the *vertical* distance of the point beneath the free surface. In Fig. 12 the pore pressures at two locations, A and B, have been calculated using this assumption.

In the context of FE analysis, the pore pressures are computed at all submerged (Gauss) points as described above, and subtracted from the *total* normal stresses computed at the same locations following the application of surface and gravity loads. The resulting *effective* stresses are then used in the

remaining parts of the algorithm relating to the assessment of Mohr–Coulomb yield and elasto-plastic stress redistribution. Note that the gravity loads are computed using *total* unit weights of the soil.

The external loading due to the reservoir is modelled by applying a normal stress to the face of the slope equal to the water pressure. Thus, as shown in Fig. 13, the applied stress increases linearly with water depth and remains constant along the horizontal foundation level. These stresses are converted into equivalent nodal loads on the FE mesh (e.g. Smith & Griffiths, 1998) and added to the initial gravity loading.

Example 5: Homogeneous slope with horizontal free surface

Figure 14 shows a similar slope to that analysed in example 1, but with a horizontal free surface at a depth L below the crest. Using the method described above, the factor of safety of the slope has been computed for several different values of the draw-down ratio (L/H), which has been varied from -0.2 (slope completely submerged with the water level

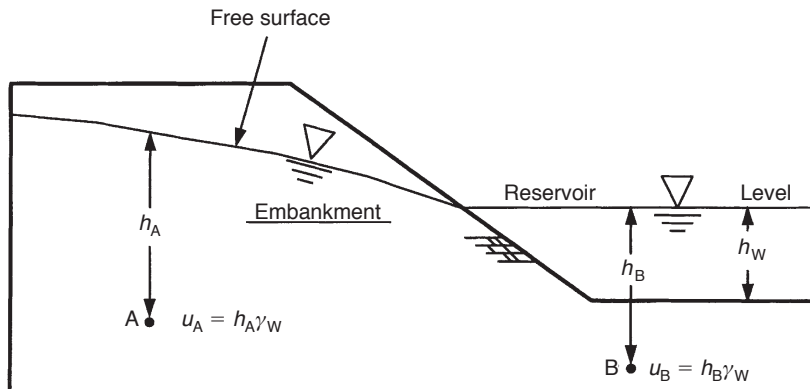


Fig. 12. Slope with free surface and reservoir loading

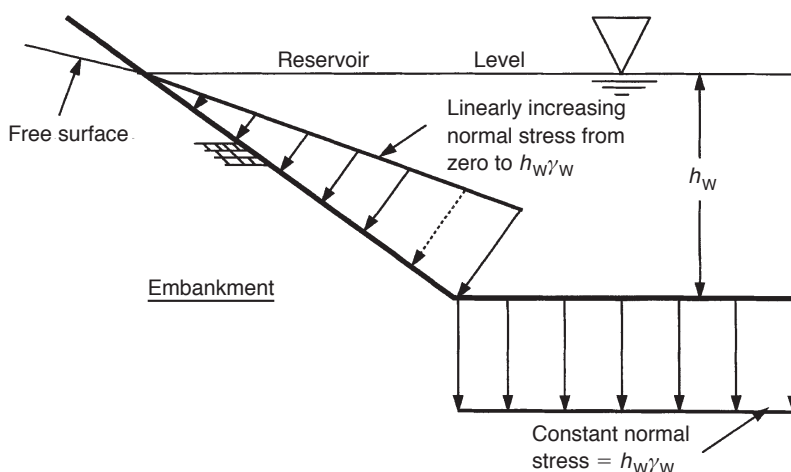


Fig. 13. Detail of submerged area of slope beneath free-standing reservoir water showing stresses to be applied to the surface of the mesh as equivalent nodal loads

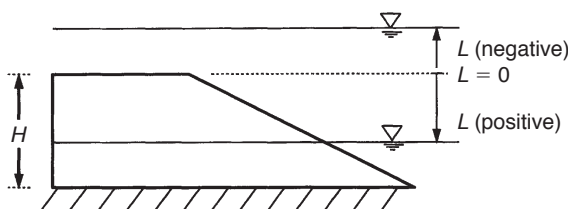


Fig. 14. Example 5: 'Slow' drawdown problem. Homogeneous slope with a horizontal free surface. Slope angle 26.57° (2:1), $\phi' = 20^\circ$, $c'/\gamma H = 0.05$ (above and below free surface)

0.2H above the crest), to 1.0 (water level at the base of the slope). The problem could be interpreted as a 'slow' drawdown problem in which a reservoir, initially above the crest of the slope, is gradually lowered to the base, with the water level within the slope maintaining the same level. A constant total unit weight has been assigned to the entire slope, both above and below the water level.

The interesting result shown in Fig. 15 indicates that the factor of safety reaches a *minimum* of $\text{FOS} \approx 1.3$ when $L/H \approx 0.7$. A limit equilibrium solution shown on the same figure indicates a similar trend (e.g. Cousins, 1978). The special cases corresponding to $L/H = 0$ and $L/H = 1$ agree well with chart solutions given, respectively, by Morgenstern (1963) ($F = 1.85$), and Bishop & Morgenstern (1960) ($\text{FOS} = 1.4$). The fully submerged slope ($L/H \leq 0$) is more stable than the 'dry' slope ($L/H \geq 1$), as indicated by a higher factor of safety.

An explanation of the observed minimum is due to the cohesive strength of the slope (which is unaffected by buoyancy) and the trade-off between soil weight and soil shear strength as the drawdown level is varied. In the initial stages of drawdown ($L/H < 0.7$), the increased weight of the slope has a proportionally greater destabilizing effect than the increased frictional strength, and the factor of safety falls. At higher drawdown levels ($L/H > 0.7$), how-

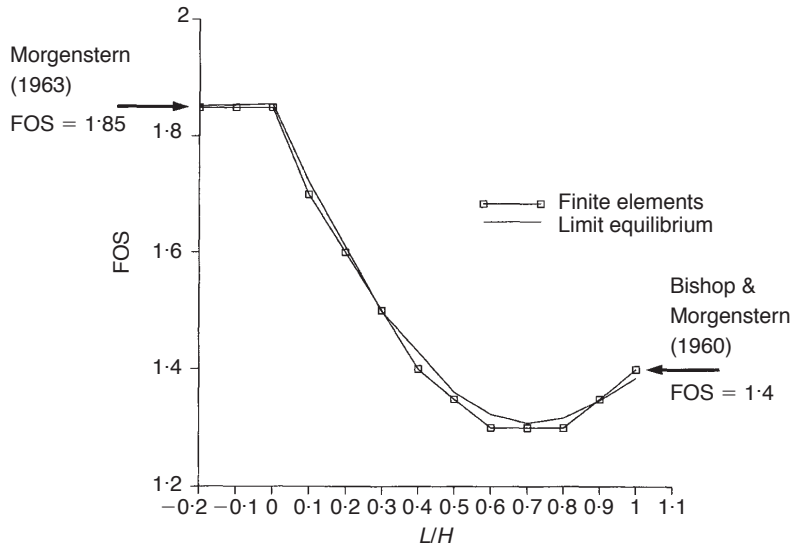


Fig. 15. Example 5: Factor of safety in 'slow' drawdown problem for different values of the drawdown ratio L/H

ever, the increased frictional strength starts to have a greater influence than the increased weight, and the factor of safety rises. Other results of this type have been reported by Lane & Griffiths (1997) for a slope which was stable ($FOS > 1$) when 'dry' or fully submerged, but became unstable ($FOS < 1$) at a critical value of the drawdown ratio L/H . It should also be pointed out from the horizontal part of the graph in Fig. 15, corresponding to $L/H \leq 0$, that the factor of safety for a fully submerged slope is unaffected by the depth of water above the crest.

Excellent agreement with Morgenstern (1963)

for 'rapid drawdown' problems has also been demonstrated for a range of slopes using a similar approach (Lane & Griffiths, 1997).

Example 6: Two-sided earth embankment

The example given in Fig. 16 is of an actual earth dam cross-section including a free surface which slopes from the reservoir level to foundation level on the downstream side (Torres & Coffman, 1997). For the purposes of this example, the material properties have been made homogeneous. Fig. 17

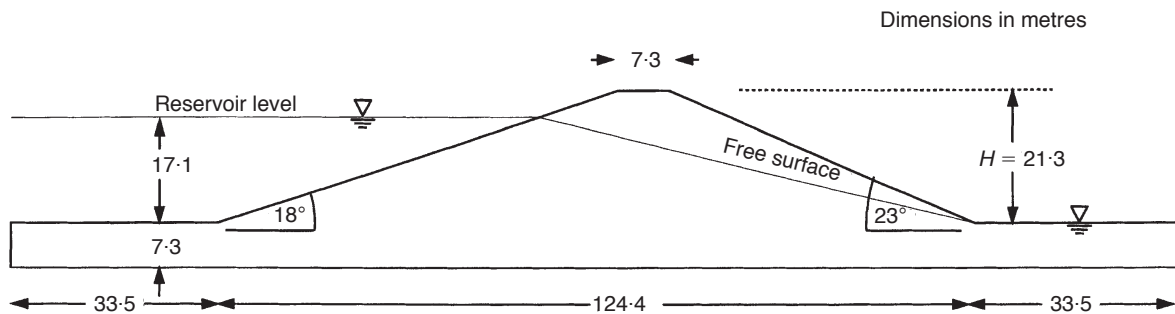


Fig. 16. Example 6: Two-sided earth embankment with a sloping free surface. Homogeneous dam, $\phi' = 37^\circ$, $c' = 13.8 \text{ kN/m}^2$, $\gamma = 18.2 \text{ kN/m}^3$ (above and below WT)

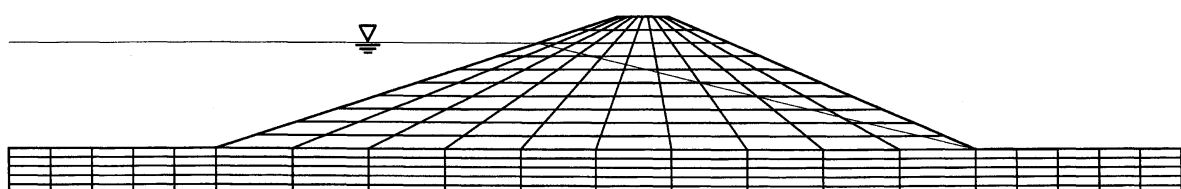


Fig. 17. Example 6: Finite element mesh

shows the FE model used for the slope stability analysis (Paice, 1997). The boundary conditions consist of vertical rollers on the faces at the left and right ends of the foundation layer with full fixity at the base. It should be noted that the downstream slope of the embankment is slightly steeper than the upstream slope.

A second analysis was also performed with no free surface corresponding to the embankment before the reservoir was filled. FE slope stability analysis led to the results shown in Fig. 18. Both cases were also solved using a conventional limit equilibrium approach which gave $FOS = 1.90$ with a free surface and $FOS = 2.42$ without a free surface. The limit equilibrium and FE factors of safety values were in close agreement in both cases.

Regarding the critical mechanisms of failure, Figs 19 and 20 show the deformed mesh corresponding to the unconverged FE solution as compared with the slip circle that gave the lowest factors of safety from the limit equilibrium approach. As expected, the lowest factor of safety occurs on the steeper, downstream side of the embankment in both cases. It should also be noted that both the FE and limit equilibrium results indicate a toe failure for the case with no free surface (Fig. 19), and a deeper mechanism extending into the foundation layer for the case with a

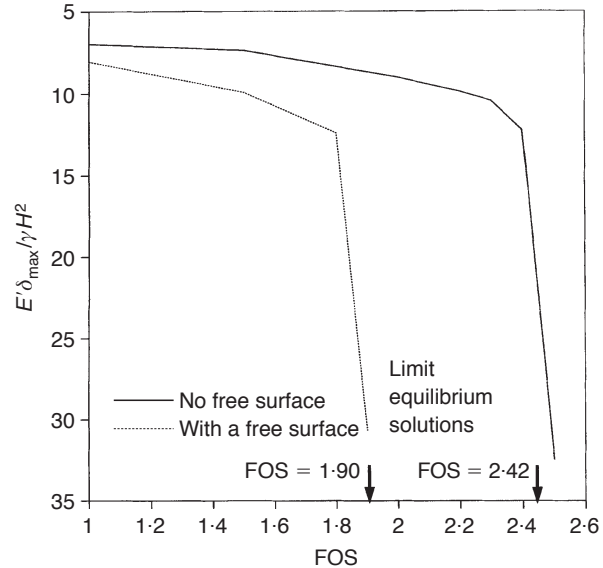


Fig. 18. Example 6: FOS versus dimensionless displacement

free surface (Fig. 20). Fig. 21 shows the corresponding displacement vectors from the FE solutions. Reasonably good agreement between the locations of the failure mechanisms by both types of analysis is indicated.

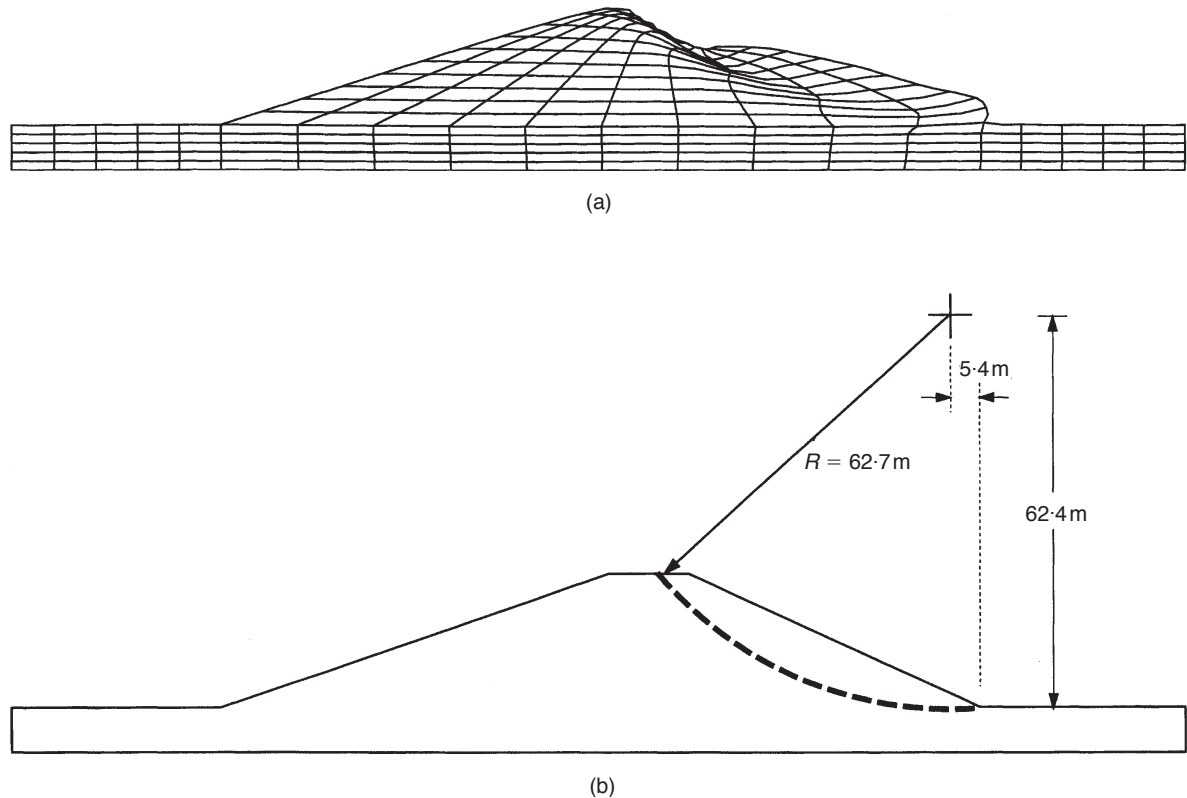


Fig. 19. Example 6 with no free surface: (a) deformed mesh corresponding to the unconverged solution by finite elements; (b) the critical slip circle by limit equilibrium. Both methods give $FOS = 2.4$

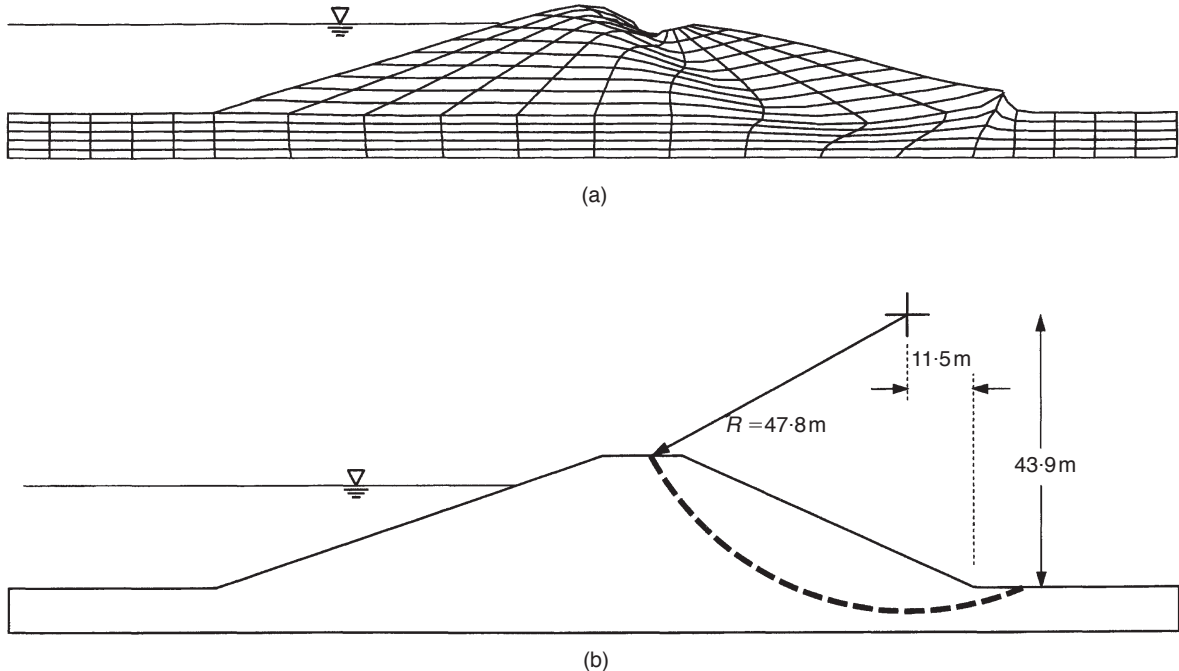


Fig. 20. Example 6 with a free surface: (a) deformed mesh corresponding to the unconverged solution by finite elements; (b) the critical slip circle by limit equilibrium. Both methods give FOS = 1.9

THE CRITERIA FOR COMPUTER-AIDED ANALYSIS

Whitman & Bailey (1967) looked forward to the future of computer-aided analysis for engineers and set criteria by which it could be judged. Their comments were originally addressed to the automation of limit equilibrium methods, but they also commented on the then emerging numerical analysis techniques.

They judged that the system must be sufficiently accurate for confidence in its use and appropriate

for the parameters being input. FE analysis meets these criteria with a degree of accuracy decided by the engineer in designing the model.

It should be possible, in a realistic timescale, to do sufficient trials to examine all the key modes of behaviour; to consider different times in the life of the structure and to vary parameters during design to test options for cost and efficiency. All this is now possible with FE methods.

Finally, the method of human-machine commu-

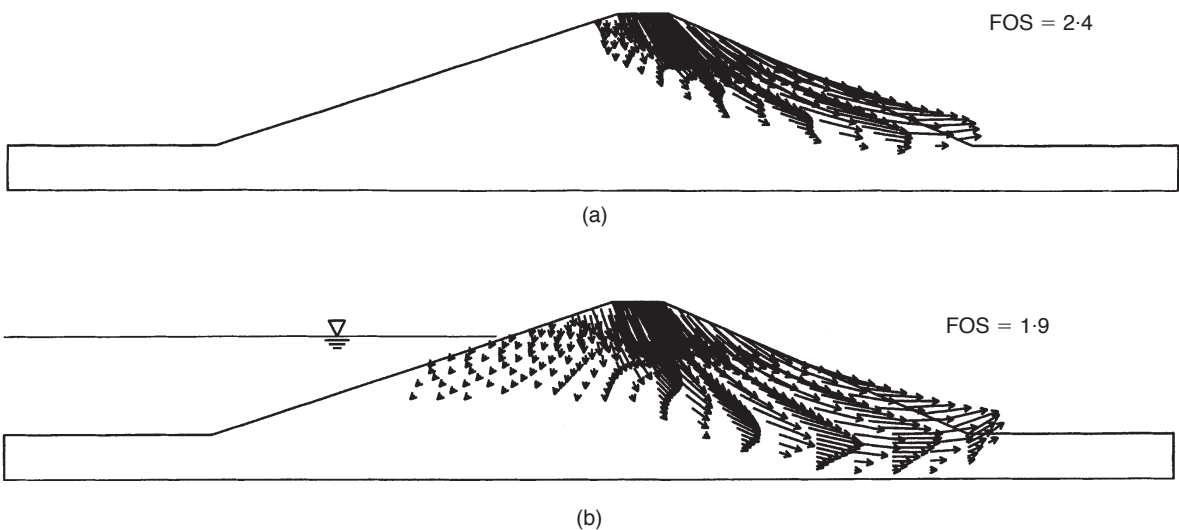


Fig. 21. Example 6: Displacement vectors corresponding to the unconverged solution by finite elements: (a) no free surface; (b) with a free surface. Only those displacement vectors that have a magnitude > 10% of the maximum are shown

nification must be user-friendly and readily accessible. This is partly a matter of program design but easily achieved. Graphical output greatly enhances the process of design and analysis over and above that from the numerical results.

Similarly, Chowdhury (1981), in his discussion of Sarma (1979), commented on the perceived reluctance to develop alternatives to limit equilibrium methods for practice when the tools to do so were already available. Since then, numerous applications and experience have verified the possibilities offered by finite elements.

The key issues of cost and turnaround time have been overtaken by the falling cost of powerful hardware and processor speeds which now make the FE method available to engineers at less than the cost of their CAD systems. What remains is the concern of powerful tools used wrongly. That is no more true of finite elements after years of application than of limit equilibrium methods, which can themselves produce seriously misleading results. Engineering judgement is still essential, whichever method is being used.

CONCLUDING REMARKS

The FE method in conjunction with an elastic–perfectly plastic (Mohr–Coulomb) stress–strain method has been shown to be a reliable and robust method for assessing the factor of safety of slopes. One of the main advantages of the FE approach is that the factor of safety emerges naturally from the analysis without the user having to commit to any particular form of the mechanism *a priori*.

The FE approach for determining the factor of safety of slopes has satisfied the criteria for effective computer-aided analysis. The widespread use of this method should now be seriously considered by geotechnical practitioners as a more powerful alternative to traditional limit equilibrium methods.

ACKNOWLEDGEMENTS

The writers acknowledge the support of NSF Grant No. CMS 97-13442. Dr Lane was supported by the Peter Allen Scholarship Fund of UMIST.

REFERENCES

Abramson, L. W., Lee, T. S., Sharma, S. & Boyce, G. M. (1995). *Slope stability and stabilisation methods*. Chichester: Wiley.

Bishop, A. W. (1955). The use of the slip circle in the stability analysis of slopes. *Géotechnique* **5**, No. 1, 7–17.

Bishop, A. W. & Morgenstern, N. R. (1960). Stability coefficients for earth slopes. *Géotechnique* **10**, 129–150.

Borja, R. I., Lee, S. R. & Seed, R. B. (1989). Numerical simulation of excavation in elasto-plastic soils. *Int. J. Numer. Anal. Methods Geomech.* **13**, No. 3, 231–249.

Chowdhury, R. N. (1981). Discussion on stability analysis of embankments and slopes. *J. Geotech. Engng. ASCE* **107**, 691–693.

Clough, R. W. & Woodward, R. J. (1967). Analysis of embankment stresses and deformations. *J. Soil. Mech. Found. Div. ASCE* **93**, SM4, 529–549.

Cousins, B. F. (1978). Stability charts for simple earth slopes. *J. Geotech. Engng. ASCE* **104**, No. 2, 267–279.

Duncan, J. M. (1996). State of the art: limit equilibrium and finite-element analysis of slopes. *J. Geotech. Engng. ASCE* **122**, No. 7, 577–596.

Duncan, J. M. & Dunlop, P. (1969). Slopes in stiff fissured clays and soils. *J. Soil Mech. Found. Div. ASCE* **95**, SM5, 467–492.

Fellenius, W. (1936). Calculation of the stability of earth dams. *Proc. 2nd congr. large dams, Washington DC* **4**.

Griffiths, D. V. (1980). *Finite element analyses of walls, footings and slopes*. PhD thesis, University of Manchester.

Griffiths, D. V. (1982). Computation of bearing capacity factors using finite elements. *Géotechnique* **32**, No. 3, 195–202.

Griffiths, D. V. (1989). Computation of collapse loads in geomechanics by finite elements. *Ing Arch* **59**, 237–244.

Griffiths, D. V. (1990). Failure criterion interpretation based on Mohr–Coulomb friction. *J. Geotech. Engng. ASCE* **116**, GT6, 986–999.

Griffiths, D. V. & Kidger, D. J. (1995). Enhanced visualization of failure mechanisms in finite elements. *Comput. Struc.* **56**, No. 2, 265–269.

Hicks, M. A. & Boughrarou, R. (1998). Finite element analysis of the Nelerk underwater berm failures. *Géotechnique* **48**, No. 2, 169–185.

Hicks, M. A. & Wong, S. W. (1988). Static liquefaction of loose slopes. *Proc. 6th Int. Conf. Numer. Methods Geomech.*, 1361–1368.

Janbu, N. (1968). Slope stability computations. *Soil Mech. Found. Engng Report*. Trondheim: Technical University of Norway.

Lambe, T. W. & Silva, F. (1995). The ordinary method of slices revisited. *Geotech. News* **13**, No. 3, 49–53.

Lambe, T. W. & Whitman, R. V. (1969). *Soil mechanics*. New York: Wiley.

Lane, P. A. & Griffiths, D. V. (1997). Finite element slope stability—why are engineers still drawing circles? *Proc. 6th Int. Symp. Numer. Models Geomech.* 589–593.

Loret, B. & Prevost, J. H. (1991). Dynamic strain localisation in fluid-saturated porous media. *J. Eng. Mech. ASCE* **117**, No. 4, 907.

Lowe, J. & Karafiath, L. (1960). Stability of earth dams upon drawdown. *Proc. 1st Pan-Am. Conf. Soil Mech. Found. Engng*, 537–552.

Matsui, T. & San, K.-C. (1992). Finite element slope stability analysis by shear strength reduction technique. *Soils Found.* **32**, No. 1, 59–70.

Molenkamp, F. (1981). *Elastic-plastic double hardening model Monot*. Technical report. Delft: Delft Geotechnics.

Morgenstern, N. R. (1963). Stability charts for earth slopes during rapid drawdown. *Géotechnique* **13**, 121–131.

Morgenstern, N. R. & Price, V. E. (1965). The analysis of the stability of general slip surfaces. *Géotechnique* **15**, No. 1, 79–93.

Naylor, D. J. (1974). Stresses in nearly incompressible

materials by finite elements with application to the calculation of excess pore pressure. *Int. J. Numer. Methods Engng* **8**, 443–460.

Naylor, D. J. & Pande, G. N. (1981). *Finite elements in geotechnical engineering*. Swansea: Pineridge Press.

Paice, G. M. (1997). *Finite element analysis of stochastic soils*. PhD thesis, University of Manchester.

Perzyna, P. (1966). Fundamental problems in viscoplasticity. *Adv. Appl. Mechanics* **9**, 243–377.

Potts, D. M., Dounias, G. T. & Vaughan, P. R. (1990). Finite element analysis of progressive failure of Carsington embankment. *Géotechnique* **40**, No. 1, 79–102.

Sarma, S. (1979). Stability analysis of embankments and slopes. *J. Geotech. Engng, ASCE* **105**, 1511–1524.

Smith, I. M. & Griffiths, D. V. (1998). *Programming the finite element method*, 3rd edn. Chichester: Wiley.

Smith, I. M. & Hobbs, R. (1974). Finite element analysis of centrifuged and built-up slopes. *Géotechnique* **24**, No. 4, 531–559.

Snitbhan, N. & Chen, W. F. (1976). Elastic–plastic large deformation analysis of soil slopes. *Comput. Struct.* **9**, 567–577.

Spencer, E. (1967). A method of analysis of the stability of embankments assuming parallel interslice forces. *Géotechnique* **17**, No. 1, 11–26.

Taylor, D. W. (1937). Stability of earth slopes. *J. Boston Soc. Civ. Eng.* **24**, 197–246.

Torres, R. & Coffman, T. (1997). *Liquefaction analysis for CAS: Willow Creek Dam*. Technical Report WL-8312-2. Denver: US Department of the Interior, Bureau of Reclamation.

Whitman, R. V. & Bailey, W. A. (1967). Use of computers for slope stability analysis. *J. Soil Mech. Found. Div., ASCE* **93**, SM4, 475–498.

Wong, F. S. (1984). Uncertainties in FE modeling of slope stability. *Comput. Struct.* **19**, 777–791.

Cormeau, I. C. (1974). Viscoplasticity, plasticity and creep in elastic solids. A unified approach. *Int. J. Numer. Methods Engng* **8**, 821–845.

Zienkiewicz, O. C., Humpheson, C. & Lewis, R. W. (1975). Associated and non-associated viscoplasticity and plasticity in soil mechanics. *Géotechnique* **25**, 671–689.

Zienkiewicz, O. C., Huang, M. & Pastor, M. (1995). Localization problems in plasticity using finite elements with adaptive remeshing. *Int. J. Numer. Anal. Methods Geomech.* **19**, No. 2, 127–148.

Zienkiewicz, O. C. & Taylor, R. L. (1989). *The finite element method*, Vol. 1, 4th edn. London, New York: McGraw-Hill.